ORGANIC CHEMISTRY

Full-nitro-nitroamino cooperative action: Climbing the energy peak of benzenes with enhanced chemical stability

Qi Sun[1], Ning Ding[1], Chaofeng Zhao[1], Qi Zhang[2], Shaowen Zhang[3], Shenghua Li[1]*, Siping Pang[1]*

More nitro groups accord benzenes with higher energy but lower chemical stability. Hexanitrobenzene (HNB) with a fully nitrated structure has stood as the energy peak of organic explosives since 1966, but it is very unstable and even decomposes in moist air. To increase the energy limit and strike a balance between energy and chemical stability, we propose an interval full-nitro-nitroamino cooperative strategy to present a new fully nitrated benzene, 1,3,5-trinitro-2,4,6-trinitroaminobenzene (TNTNB), which was synthesized using an acylation-activation-nitration method. TNTNB exhibits a high density (*d*: 1.995 g cm^{-3} at 173 K, 1.964 g cm^{-3} at 298 K) and excellent heat of detonation (*Q*: 7179 kJ kg^{-1}), which significantly exceed those of HNB (*Q*: 6993 kJ kg^{-1}) and the state-of-the-art explosive CL-20 (*Q*: 6534 kJ kg^{-1}); thus, TNTNB represents the new energy peak for organic explosives. Compared to HNB, TNTNB also exhibits enhanced chemical stability in water, acids, and bases.

INTRODUCTION

Since the discovery of benzene by Faraday nearly 200 years ago, the functionalization of benzene has been rapidly developing, owing to the structurally diverse benzene derivatives that can be generated by replacing the six hydrogen atoms with functional substituents (*1*–*3*). Polysubstituted benzenes have received widespread attention and have indispensable applications in chemistry and materials fields (*4*–*6*). For example, polynitrobenzenes are important intermediates in the synthesis of amino or azo functional compounds, which are widely used as medicines, pesticides, and dyes (*7*, *8*). Polynitrobenzenes are also well-known high-energy-density materials (HEDMs) (Fig. 1A), which contain oxidizers (nitro groups) and fuel components (benzene ring) within a single molecule and generate energy rapidly through self-redox reactions. Consequently, these compounds play important roles in pyrotechnics, mining engineering, aerospace exploration, and most modern defense systems (*9*–*16*). The most representative energetic polynitrobenzenes are 2,4,6-trinitrotoluene (TNT; 1863, the most famous explosive) and hexanitrobenzene (HNB; 1966, the only fully nitrated benzene) (*14*–*18*). Generally, the energy of these materials progressively increases with an increasing number of nitro groups in the benzene ring (Fig. 1A). For example, the heat of detonation (*Q*), which reflects the power output upon explosion, is 3054 kJ kg^{-1} for nitrobenzene (one nitro group) and 4247 kJ kg^{-1} for TNT (three nitro groups) (*13*–*17*). Particularly, benzene, which is fully substituted with six nitro groups (i.e., HNB), has exhibited the highest energy (*Q*: 6993 kJ kg^{-1}) among the organic explosives since 1966. In addition, HNB has other excellent energetic properties, such as high density (*d*: 1.98 g cm^{-3}) and high detonation velocity (*D*: 9277 m s^{-1}) (*17*–*20*).

However, an increase in the number of nitro groups in the benzene ring usually results in lower chemical stability (*12*–*18*). For instance, TNT (three nitro groups) is highly stable and is still widely used for national defense purposes (*14*–*16*). In contrast, HNB (six nitro groups) exhibits a higher energy than TNT but has poor chemical stability and decomposes rapidly in moist air, thereby limiting its practical application (*21*–*25*). With an increasing number of nitro groups, the number of hydrogen bond acceptors (-NO_2) increases, whereas the number of hydrogen bond donors (hydrogen atoms) of the benzene ring decreases, thus weakening the intramolecular hydrogen bonding interactions. Furthermore, the aromaticity of the benzene ring decreases, resulting in lower stability. Over the past decades, research has mostly focused on improving the stability of HNB by transforming its partial nitro groups into other functional groups and developing new explosives such as 1,3,5-trinitro-2,4,6-triaminobenzene (TATB) (*Q*: 3858 kJ kg^{-1}) and 1,3,5-trinitro-2,4,6-trihydroxylbenzene (*Q*: 3991 kJ kg^{-1}). Although these compounds exhibit increased chemical stability, their energy decreases significantly compared with that of HNB (*11*–*15*). To date, striking a balance between energy and chemical stability, as well as further increasing the energy and improving the stability of polynitrobenzenes simultaneously, is a notable challenge.

Similar to the nitro group, the nitroamino group (-$NHNO_2$) is one of the most frequently used energetic groups in the design of HEDMs. In addition to a nitro unit (Fig. 1B), this group contains an additional high-energy N—N bond; thus, its introduction can effectively increase the density and heat of formation, affording compounds with higher energy (*26*–*30*). Furthermore, the nitroamino group has an imino group (N—H), which can provide a hydrogen bond donor, and the nitrogen atom of the imino group has lone pair electrons that potentially form p-π conjugation. Considering these attractive features of the nitro and nitroamino groups, we propose an interval full-nitro-nitroamino cooperative strategy to design a new fully nitrated benzene, 1,3,5-trinitro-2,4,6-trinitroaminobenzene (TNTNB), by replacing the three interval nitro groups of HNB with three nitroamino groups (Fig. 1B). We speculated that this strategy would result in a higher energy and better chemical stability of TNTNB compared with those of HNB. The reasons for this speculation are as follows: (i) similar to HNB, TNTNB has six nitro groups; moreover, it contains three additional high-energy N—N bonds, which could act cooperatively to endow better energetic performance; (ii) unlike HNB, TNTNB has three interval N—H groups that could cooperatively form intramolecular hydrogen bonds with adjacent -NO_2

[1]School of Materials Science and Engineering, Beijing Institute of Technology, Beijing 100081, China. [2]Institute of Chemical Materials, China Academy of Engineering Physics (CAEP), Mianyang 621050, China. [3]School of Chemistry and Chemical Engineering, Beijing Institute of Technology, Beijing 100081, China.
*Corresponding author. Email: lishenghua@bit.edu.cn (S.L.); pangsp@bit.edu.cn (S.P.)

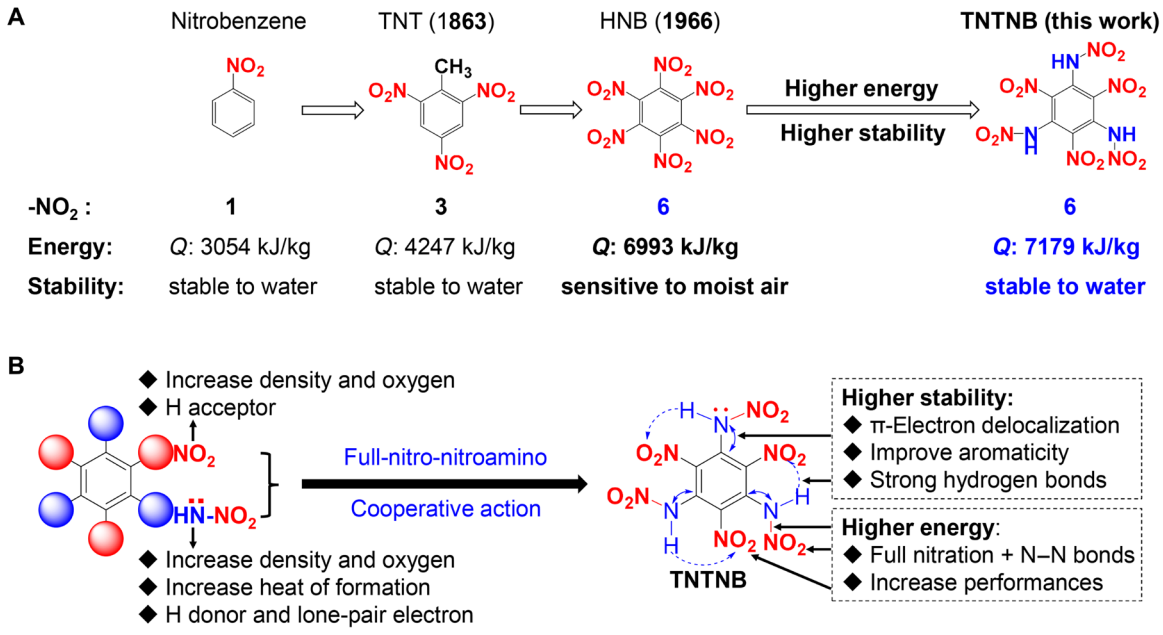

Fig. 1. The background of nitro-benzenes and design strategy of TNTNB. (**A**) Comparison of the number of -NO_2 groups, energy (*Q*: heat of detonation), and stability (chemical stability) of nitrobenzene, TNT, HNB, and TNTNB, respectively. (**B**) Design of TNTNB through interval full-nitro-nitroamino cooperative action.

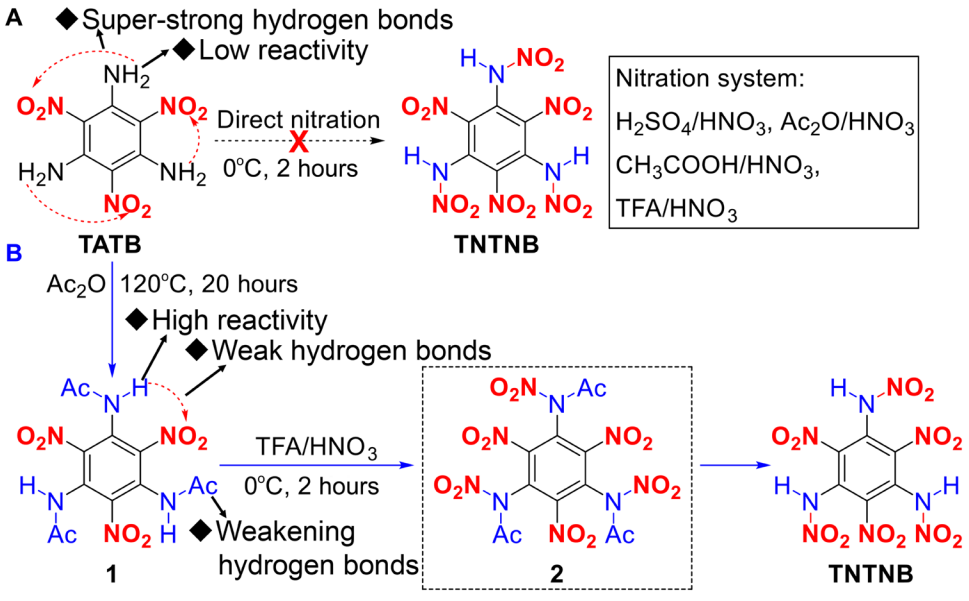

Fig. 2. Synthesis of TNTNB. (**A**) Unsuccessful nitration from TATB to TNTNB using various nitration systems. (**B**) Synthesis of TNTNB using the proposed acylation-activation-nitration strategy.

groups, thus enhancing the chemical stability; and (iii) the nitrogen atoms of the three interval imino groups in TNTNB could form a large p-π conjugated system with the benzene ring and increase its aromaticity, thereby further enhancing its stability.

RESULTS

Synthesis of TNTNB via an acylation-activation-nitration method

First, the preparation of TNTNB was explored. One-step nitration of amino groups is a common method for introducing nitroamino groups (Fig. 2A). Thus, we attempted the direct nitration of TATB, an easily available compound, using various nitrate systems [e.g., H_2SO_4/HNO_3, Ac_2O/HNO_3, AcOH/HNO_3, and CF_3COOH (TFA)/HNO_3] to obtain the target compound. Unfortunately, all the attempts failed, and the starting materials were recovered. This is mainly because the extremely strong intramolecular hydrogen bonds (Fig. 3, A and E) passivate the amino groups of TATB, resulting in low reactivities (*31*, *32*). This may also explain why TATB has not been successfully nitrated to date since it was first prepared in 1888 (*33*).

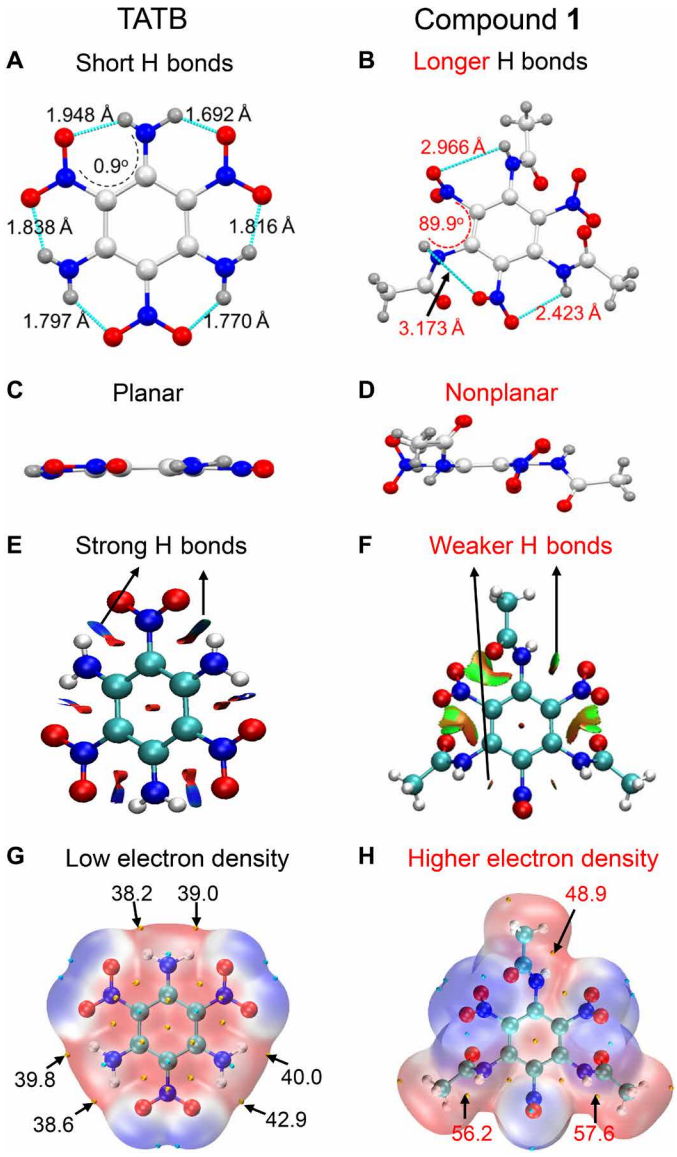

Fig. 3. Mechanism investigation of the acylation-activation-nitration method through x-ray data and quantum computing. (**A** and **B**) Crystal structure comparison of TATB (*44*) and compound **1** showing the hydrogen bond lengths and partial torsion angles; green dashed lines indicate hydrogen bonds. (**C** and **D**) Planar structure of TATB and nonplanar structure of compound **1**. Atom color: blue, N; red, O; white, C; gray, H. (**E** and **F**) Calculated intramolecular hydrogen-bonding interactions in TATB and compound **1** by noncovalent interaction analysis using Gaussian 09 (*45*) and Multiwfn (*46*) programs. Blue, strong intramolecular attractive interaction; green, weak intramolecular attractive interactions. (**G** and **H**) Electrostatic surface potential (ESP)–mapped molecular van der Waals (vdW) surfaces of TATB and compound **1**. Surface local minima and maxima of ESP (kcal mol^{-1}) are represented as cyan and yellow spheres, respectively.

Accordingly, we envisioned that the key to accomplishing nitration of TATB was to enhance the activity of the inert amino groups. Thus, an acylation-activation-nitration method was proposed (Fig. 2B). In this method, highly reactive acetylation reagents, such as acetic anhydride and acetyl chloride, were used to activate and acetylate TATB to produce acetamide **1**. We anticipated that the introduction of large acetyl groups to substitute a proton in the amino groups of TATB could destroy the extremely strong intramolecular interactions, thus endowing **1** with higher reactivity. Using the proposed method, when TATB was reacted with commercially available acetic anhydride at 120°C, **1** was successfully obtained in high yield. Then, when a mild nitration system (TFA/HNO_3) was used at 0°C, **1** was simultaneously nitrated and deacylated (Fig. 2B), and TNTNB was successfully obtained. TNTNB was fully characterized by elemental analysis, infrared (IR) spectroscopy, and ^{1}H, ^{13}C, and ^{15}N nuclear magnetic resonance (NMR) spectroscopy (see the Supplementary Materials).

The full nitrification of benzene is extremely challenging, and the preparation of HNB requires extremely harsh reaction conditions, including the use of ultradry solvents and dangerous chemicals such as 90% H_2O_2 or 30% SO_3/H_2SO_4 (*21*–*25*). However, because the acylation-activation-nitration method was used, the synthetic conditions for TNTNB were milder than those for HNB. Moreover, the successful synthesis of TNTNB demonstrated the effectiveness of this proposed synthetic strategy for solving a long-standing (since 1888) problem: the nitration of inert TATB with extremely strong hydrogen-bonding interactions.

To determine the difference in reactivity between TATB and **1**, single-crystal x-ray data of **1** were obtained, and their intramolecular hydrogen-bonding interactions were investigated. As shown in Fig. 3, the interval amino and nitro groups force TATB to exhibit a planar structure and have strong intramolecular hydrogen bonds with lengths of 1.692 to 1.948 Å (Fig. 3, A and C). Unlike TATB, all the nitro and NH groups in **1** were noncoplanar with the benzene ring (Fig. 3, B and D). The torsion angles in **1** ranged from 52° to 118°, whereas those in TATB were less than 5° (Fig. 3, A and B). Moreover, the lengths of the intramolecular hydrogen bonds between -NO_2 and -NH in **1** ranged from 2.432 to 3.173 Å and were longer than those in TATB (1.691 to 1.948 Å, Fig. 3, A and B). Thus, the introduction of acetyl groups into TATB destroyed the extremely strong intramolecular interactions.

To further determine the weakening of hydrogen bonds, density functional theory was used to calculate the noncovalent interactions between TATB and **1**. The results (Fig. 3, E and F) showed that **1** had significantly weaker intramolecular hydrogen bonding interactions than TATB. In addition, the electrostatic potential surfaces of TATB and **1** were calculated and are shown in Fig. 3 (G and H). Nitration is a typical electrophilic substitution reaction. Therefore, the higher the electron density around the amino groups, the easier it is for the nitration reaction to proceed, that is, the higher the reactivity. It is clear that the electron densities of the imino groups in **1** (48.9 to 57.6 kcal mol^{-1}) are higher than those of TATB (38.2 to 42.9 kcal mol^{-1}), which means that compound **1** is more prone to nitration. The successful nitration of TATB and investigation of its mechanism indicate that the proposed synthetic method can be a useful tool for the activation and nitration of inert amino compounds.

Structure features of TNTNB

To further confirm the structure of TNTNB and investigate its structure-property relationships, anhydrous TNTNB crystals suitable for x-ray single-crystal diffraction were obtained in situ from the reaction system. TNTNB crystallized in the monoclinic space group $P2_1/c$, contained four molecules in the unit cell, and had an extremely high density of 1.995 g cm^{-3} at 173 K. It should be noted that TNTNB is the second known hexanitro-containing benzene derivative. Similar to HNB (*34*), TNTNB adopted a nonplanar molecular structure, owing to the mutual repulsion and steric hindrance between the

poly-nitro groups (Fig. 4, A and B). However, the lengths of the C—C bonds in the benzene ring were more uniform than those in HNB; the difference between the shortest (1.387 Å) and longest (1.400 Å) bonds was 0.013 Å, which was significantly smaller than the difference (0.062 Å) between the shortest (1.406 Å) and longest (1.344 Å) bonds in HNB. Thus, the smaller difference for TNTNB corresponds to a higher aromaticity than that of HNB.

To further confirm the higher aromaticity of TNTNB than that of HNB, the GIAO/B3LYP/6-311++G** method was used to calculate their nucleus independent chemical shifts (NICSs), a commonly used parameter to describe the aromaticity of a compound (*35*). The results showed that the NICS(1)$_{zz}$ value of TNTNB was −22.1 ppm, which is higher than that of HNB (−19.8 ppm), indicating that TNTNB exhibited stronger magnetic field shielding and stronger aromaticity. The aromaticity of HNB and TNTNB can be demonstrated more intuitively using the shielding maps (Fig. 4, C and D); the darker red color of the ring indicates higher aromaticity of the structure (*36*). The red color of the benzene ring in TNTNB was much darker than that in HNB, thus indicating higher aromaticity. Moreover, the π-electron delocalization behaviors of TNTNB and HNB were calculated. In general, the better the π-electron delocalization, the higher the aromaticity. On the basis of the localized orbital locator (LOL) theory (*37*), the π-electron isosurfaces with a value of 0.40 for these two compounds were visualized using the Multiwfn program. As shown in Fig. 4 (E and F), the LOL-π isosurfaces on both benzene rings are connected. However, in HNB, the LOL-π isosurface of the benzene ring was disconnected from all the nitro groups, whereas the isosurface of the nitroamino groups in TNTNB was connected to the benzene ring through the imino groups. This indicates that TNTNB had stronger π-electron delocalization than HNB. As expected, the nitrogen atoms of N—H in TNTNB had lone pair of electrons and formed a p-π conjugated system with the benzene ring, resulting in stronger π-electron delocalization and higher aromaticity.

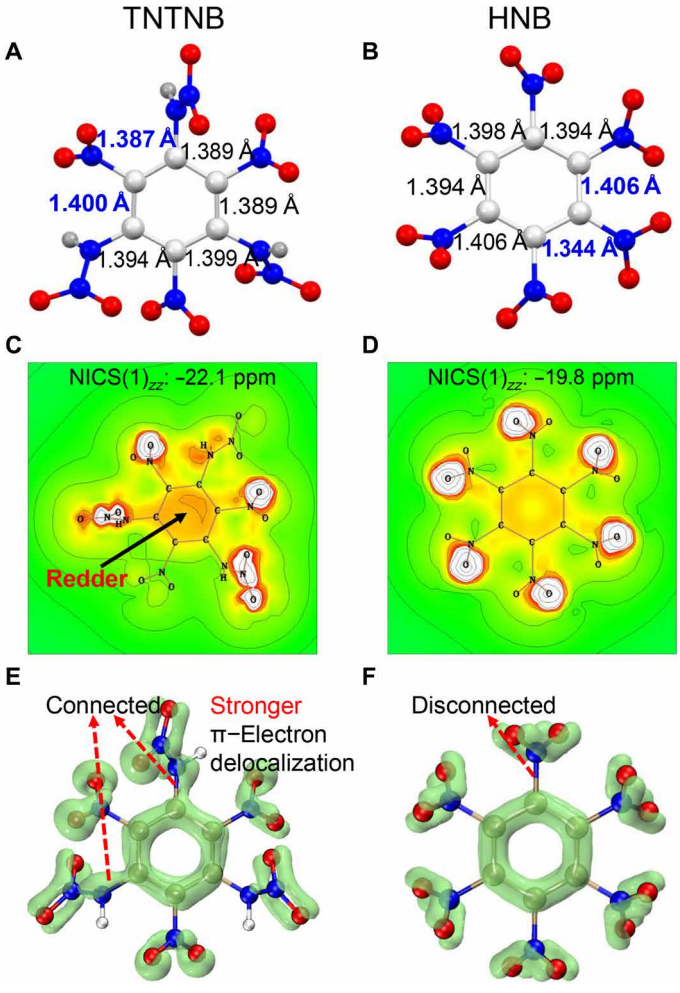

Fig. 4. Crystal structures and aromaticity features of TNTNB compared with HNB. (**A** and **B**) Single-crystal x-ray structures for TNTNB and HNB showing the C—C bond lengths in benzene rings. (**C** and **D**) Magnetic field shielding maps for TNTNB and HNB based on the NICS (nucleus independent chemical shift) method. (**E** and **F**) π-Electron delocalization for TNTNB and HNB based on the localized orbital locator (LOL) theory under an isosurface with same value (0.40).

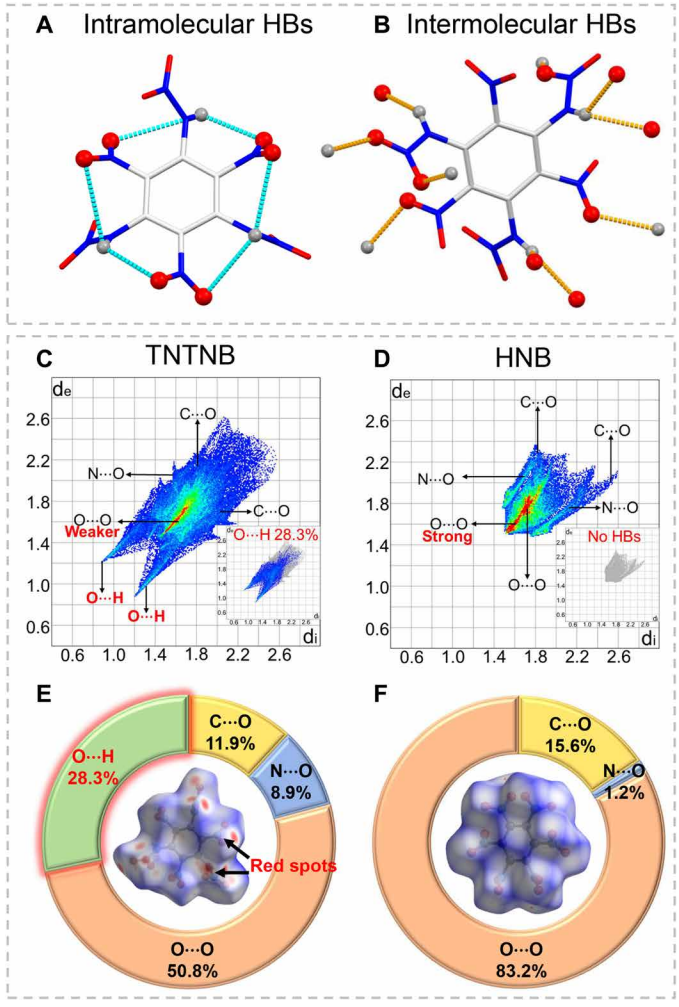

Fig. 5. Hydrogen-bonding interactions of TNTNB and noncovalent interaction analysis of TNTNB compared with HNB. (**A**) Intramolecular hydrogen bonds (HBs) in TNTNB; blue dashed lines indicate intramolecular HBs. (**B**) Intermolecular HBs in TNTNB; orange dashed lines indicate intermolecular HBs. (**C** and **D**) Highlighting O···H contacts (inside) and 2D fingerprint plots in crystal stacking for TNTNB and HNB. (**E** and **F**) Hirshfeld surfaces (inside) and pie graphs for TNTNB and HNB showing the percentage contribution of the individual atomic contacts to the Hirshfeld surfaces.

Table 1. Physical and energetic properties of TNTNB and its salts (3 and 4) in comparison with the representative energetics, namely, TNT, HNB, HMX, CL-20, DDNP, and LA. HMX, octogen; CL-20, hexanitro-aza-iso-wurzitane; DDNP, diazodinitrophenol; LA, lead azide.

Compound	d*	H_f†	Q‡	D§	T_d‖	IS¶	FS#	ESD**
TNTNB	1.964	1.00	7179	9510	65	1	5	5
3	1.821	−0.42	5513	8645	159	2	10	20
4	1.885	0.61	6132	9235	180	4	40	80
TNT††	1.650	−0.26	4247	6881	290	15	350	460
HNB‡‡	1.980	0.22	6993	9277	246	–	–	–
HMX§§	1.905	0.25	5796	9144	279	7.4	120	200‖‖
CL-20§§	2.040	0.84	6534	9445	215	4	48	130‖‖
DDNP¶¶	1.720	1.55	5009	6900	158	1	24.7	1.8
LA¶¶	4.800	1.53	1561	5920	315	2.5–4	0.1–1	6–12

*Density measured by gas pycnometer at 25 °C, g cm^{-3}. †Heat of formation, kJ g^{-1}. ‡Heat of detonation, kJ kg^{-1}. §Detonation velocity, m s^{-1}.
‖Decomposition temperature, °C. ¶Impact sensitivity, J. #Friction sensitivity, N. **Electrostatic discharge sensitivity, mJ.
††(*14*). ‡‡(*19*, *20*). §§(*28*). ‖‖(*48*). ¶¶(*49*).

Another notable feature of the crystal structures of TNTNB and HNB is the difference in their hydrogen bonds. As shown in Fig. 5 (A and B), the -NO_2 groups and the N—H bond of the adjacent nitroamino groups in TNTNB formed six intramolecular hydrogen bonds with bond lengths ranging from 2.372 to 3.244 Å. Moreover, each TNTNB molecule has 10 intermolecular hydrogen bonds with bond lengths in the range of 2.291 to 2.441 Å. In contrast, HNB does not have any hydrogen bonds because of the absence of hydrogen bond donors (hydrogen atoms). The CrystalExplorer program (*38*) was used to calculate the two-dimensional (2D) fingerprint and Hirshfeld surface for better quantitative analysis of the overall noncovalent interactions. As shown in Fig. 5C, typical O···H spikes were observed in the 2D fingerprint of TNTNB but were absent in that of HNB (Fig. 5D). The 2D fingerprint also revealed a weakening of the O···O effect in TNTNB relative to that in HNB, as is evident from the smaller red area (Fig. 5, C and D). Quantitative analysis of the overall noncovalent interactions (Fig. 5, E and F) indicated an effective reduction in the unfavorable O···O interactions from 83.2% (HNB) to 50.8% (TNTNB) and a marked increase in the O···H (hydrogen bond) interactions from 0% (HNB) to 28.3% (TNTNB). Furthermore, the Hirshfeld surface of TNTNB had more red spots (Fig. 5, E and F), further confirming the stronger hydrogen bonding interactions in TNTNB than in HNB. Thus, the introduction of interval nitroamino groups into TNTNB facilitated extensive hydrogen-bonding interactions.

Energetic performance of TNTNB

Owing to the fully nitrated benzene structure and three additional high-energy N—N bonds, the energetic performance of TNTNB was investigated (Table 1). Gas pycnometry revealed that TNTNB had an extremely high density of 1.964 g cm^{-3} at 25°C. Although this value is slightly lower than that of HNB (1.980 g cm^{-3}), it is significantly higher than those of TNT (1.650 g cm^{-3}) and octogen (HMX) (1.905 g cm^{-3}). Meanwhile, Gaussian 09 calculations revealed that the heat of formation of TNTNB was 1.00 kJ g^{-1}, which is much higher than those of HNB (0.22 kJ g^{-1}), TNT (−0.26 kJ g^{-1}), HMX (0.25kJ g^{-1}), and CL-20 (0.84 kJ g^{-1}); this was mainly attributed to the three additional high-energy N—N bonds in TNTNB. Using the density and heat of formation, the detonation performance of this typical CHON energetic compound was evaluated using the classical Kamlet-Jacobs (K-J) equation (*39*) (see the Supplementary Materials). TNTNB exhibited a significantly higher heat of detonation (Q: 7179 kJ kg^{-1}) and detonation velocity (D: 9510 m s^{-1}), which are higher than those of HNB (Q: 6993 kJ kg^{-1} and D: 9277 m s^{-1}) and the state-of-the-art explosive CL-20 (Q: 6534 kJ kg^{-1} and D: 9445 m s^{-1}). Furthermore, its heat of detonation is equal to that of 1.69 equivalent for TNT, which is obviously higher than the TNT equivalent of CL-20 (1.54 equivalent of TNT). To the best of our knowledge, the heat of detonation of TNTNB is the highest among the organic explosives (Fig. 6). Thus, the full-nitro-nitroamino cooperative strategy could provide fresh insights into the design of new materials with super-high energy.

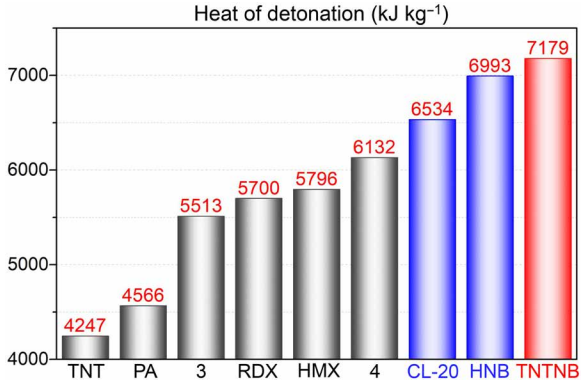

Fig. 6. Heats of detonation (energy) of TNTNB and some representative energetic compounds (*47*). PA, 2,4,6-trinitrophenol; RDX, hexogen; HMX, octogen; CL-20, hexanitro-aza-iso-wurzitane.

Chemical stability in water, acids, and bases

The higher aromaticity and stronger intramolecular hydrogen bonding interactions in TNTNB motivated us to investigate its chemical

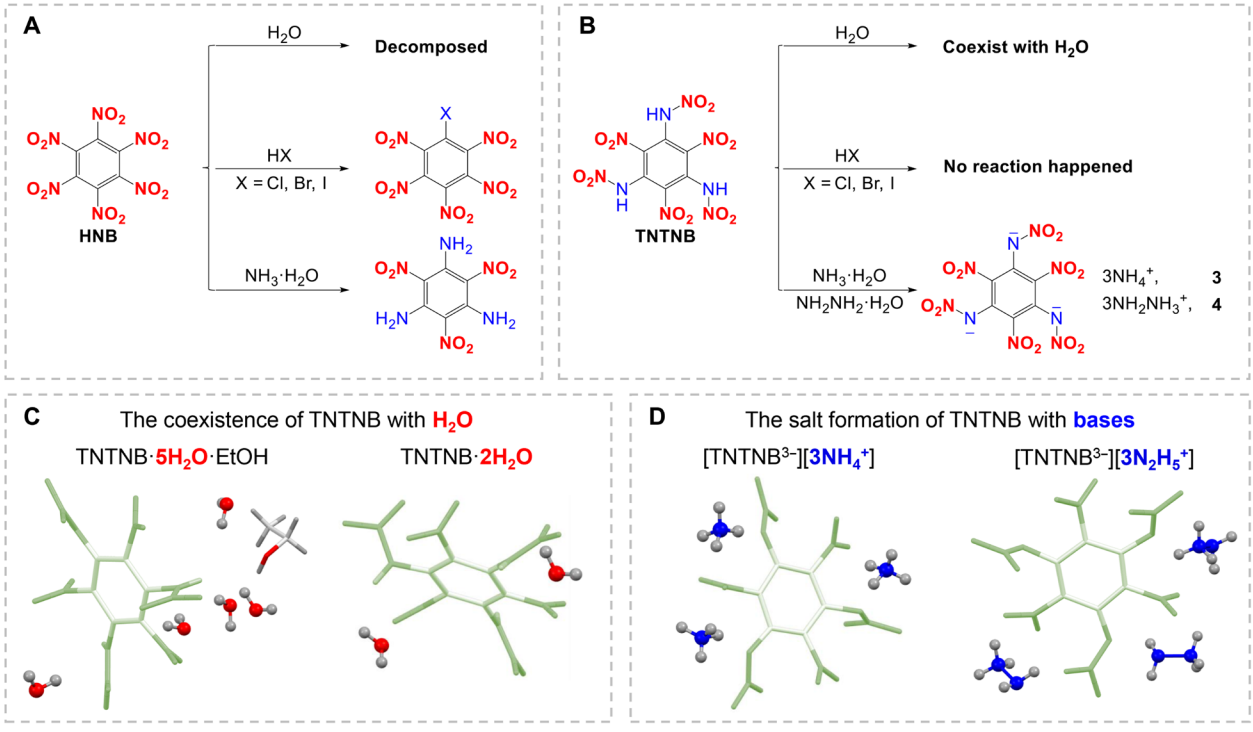

Fig. 7. Chemical stability of HNB and TNTNB with water, acids, and bases, respectively. (**A**) Chemical stability of HNB. (**B**) Chemical stability of TNTNB. (**C**) Single-crystal x-ray structural confirmation of chemical stability of TNTNB with H_2O, namely, TNTNB·5H_2O·EtOH and TNTNB·2H_2O. (**D**) Single-crystal x-ray structural confirmation of chemical stability of TNTNB with bases, namely, [$TNTNB^{3-}$][$3NH_4^+$] (compound **3**) and [$TNTNB^{3-}$][$3N_2H_5^+$] (compound **4**).

stability in water, acids, and bases (Fig. 7). Accordingly, TNTNB was dissolved in an aqueous solution of methanol, and the ^{13}C NMR spectra of this solution were monitored over time. TNTNB remained intact even after 1 month (see the Supplementary Materials). Moreover, slow evaporation of the aqueous ethanol solution in air for several days resulted in the formation of several crystals. Single-crystal x-ray diffraction analysis suggested that the formula was TNTNB·5H_2O·EtOH and that one TNTNB molecule could coexist with five H_2O molecules (Fig. 7C). In addition, another dihydrate, TNTNB·2H_2O, was obtained from its chloroform solution (Fig. 7C). However, when HNB comes into contact with a small amount of water or moisture, it immediately decomposes (*13*, *14*). Thus, TNTNB exhibited higher stability in water than HNB. To further explore the mechanism underlying the higher water stability of TNTNB, the reactivities of HNB and TNTNB toward water were studied using DLPNO-CCSD(T) at the cc-PVDZ level using the ORCA program (see the Supplementary Materials). The results indicated that the Gibbs free energy of TNTNB reaction with water was 39.36 kcal mol^{-1}, which is significantly higher than that of HNB (26.63 kcal mol^{-1}), further confirming the higher water stability of TNTNB.

Moreover, when TNTNB was added separately to an aqueous ammonia solution or hydrazine solution, the corresponding salts (**3** and **4**; Fig. 7B) were obtained in high yields. Their structures were confirmed using single-crystal x-ray diffraction (Fig. 7D). This is because TNTNB contains three acidic protons (N—H) that easily dissociate to form TNTNB salts with bases. In addition, hydrazinium salt **4** exhibited a good detonation velocity (*D*: 9235 m s^{-1}), which was higher than or comparable to those of HNB and HMX. By contrast, when HNB was added to an aqueous ammonia solution, the former immediately decomposed and its aminated product was partially formed (*24*). Moreover, TNTNB maintained good stability in HCl, HBr, and HI (see the Supplementary Materials). The above results showed that TNTNB had higher chemical stability than HNB, and this stability may originate from its higher aromaticity and stronger intramolecular hydrogen bonding interactions. Thus, cooperative action also enhanced the chemical stability of TNTNB.

Thermal stability and sensitivity

The thermal stability of TNTNB and its salts was also explored using differential scanning calorimetry (DSC). TNTNB exhibited relatively low thermal stability, with a decomposition temperature of 65°C. Furthermore, its thermal stability can be effectively improved by salt formation (159°C for **3** and 180°C for **4**). Different from chemical stability, the thermal stability of a compound is mainly determined by the bond dissociation energy (BDE) of its trigger bond (*40*–*43*). Theoretical calculations showed that the higher thermal stability of the salts can be attributed to the increase in BDEs for their trigger bonds. The BDE of the trigger bond for TNTNB was 153.01 kJ mol^{-1}, but those for salts **3** and **4** were much higher with values of 202.51 and 211.69 kJ mol^{-1}, respectively. In addition, the lower thermal stability compared with HNB also resulted from the higher BDE of HNB, with a value of 254.10 kJ mol^{-1}. Although HNB has higher thermal stability, its extremely poor chemical stability in humid air greatly limits its practical use. The sensitivities of TNTNB to external stimuli were also determined and showed an impact sensitivity (IS) of 1 J, a friction sensitivity (FS) of 5 N, and an electrostatic discharge sensitivity (ESD) of 5 mJ, which classifies as a primary explosive.

Salts **3** (IS: 2 J; FS: 10 N; ESD: 20 mJ) and **4** (IS: 4 J; FS: 40 N; ESD: 80 mJ) had better sensitivities than TNTNB. TNTNB was compared with representative primary explosives, namely, diazodinitrophenol (DDNP) and lead azide (LA), and the results are summarized in Table 1. TNTNB (*Q*: 7179 kJ kg^{-1}; *D*: 9510 m s^{-1}) showed much higher heat of detonation and detonation velocity than those of DDNP (*Q*: 5009 kJ kg^{-1}; *D*: 6900 m s^{-1}) and LA (*Q*: 1561 kJ kg^{-1}; *D*: 5920 m s^{-1}). In addition, the sensitivity features of TNTNB were comparable with those of DDNP (IS: 1 J; FS: 24.7 N; ESD: 1.8 mJ) and LA (IS: 2.5 to 4 J; FS: 0.1 to 1 N; ESD: 6 to 12 mJ).

DISCUSSION

In summary, a new fully nitrated benzene-based HEDM, TNTNB, was developed using an interval full-nitro-nitroamino cooperative strategy. TNTNB was successfully synthesized through an acylation-activation-nitration method, effectively addressing the long-standing (since 1888) problem of unsuccessful nitration of inert TATB. With a high density of 1.964 g cm^{-3} and an excellent heat of formation of 1.00 kJ g^{-1}, TNTNB exhibits much higher heat of detonation and detonation velocity (*Q*: 7179 kJ kg^{-1} and *D*: 9510 m s^{-1}) than those of HNB (*Q*: 6993 kJ kg^{-1} and *D*: 9277 m s^{-1}) and CL-20 (*Q*: 6534 kJ kg^{-1} and *D*: 9445 m s^{-1}), thus rendering it the new energy peak of organic explosives. X-ray single-crystal diffraction and theoretical calculations indicated that TNTNB has higher aromaticity and stronger hydrogen-bonding interactions than HNB, resulting in its higher chemical stability in water, bases, and acids. Moreover, its acidic characteristics facilitate the formation of energetic salts, effectively improving the thermal stability of TNTNB and affording diverse energetic derivatives. The successful synthesis of TNTNB will undoubtedly motivate the development of benzene-based compounds and energetic materials. Moreover, the proposed interval full-nitro-nitroamino cooperative strategy could be an effective method for the design of new HEDMs with both higher energy and enhanced stability.

MATERIALS AND METHODS

General methods

All reagents were purchased from Energy Chemical of analytical grade and were used as supplied. The melting points and decomposition temperatures were obtained on a differential scanning calorimeter (Mettler Toledo DSC823e) at a scan rate of 5°C min^{-1} in closed Al containers with a nitrogen flow of 50 ml min^{-1}. Chemical shifts in the ^{1}H and ^{13}C NMR spectra were reported relative to Me_4Si as external standards. Chemical shifts in the ^{15}N NMR spectra were reported relative to CH_3NO_2 as external standards. IR spectra were recorded using KBr pellets for solids on a Thermo Nicolet iS10 spectrometer. Elemental analyses were carried out on a vario EL III CHNOS elemental analyzer.

Safety precautions

All the new benzene compounds in this manuscript are powerful explosives and should be handled with extreme care using the best safety practices.

Synthesis details

1,3,5-Triacetylamino-2,4,6-trinitrobenzene (1)

TATB (2.58 g, 100 mmol) was dispersed into acetic anhydride (50 ml), and two drops of sulfuric acid were added into the mixture as catalyst, which was then stirred at 120°C. After reaction for 20 hours, the mixture was cooled to 25°C and poured into water (100 ml), which was then stirred at 90°C for another 1 hour. The precipitate was filtered out after the mixture was cooled to 25°C and washed with water (20 ml) and methanol (20 ml) to give **1** (2.87 g, 74.7% yield). ^{1}H NMR [dimethyl sulfoxide (DMSO)–d_6, 500 MHz]: δ 10.76 (s), 2.01 (s) ppm. ^{13}C NMR (DMSO-d_6, 125 MHz): δ 170.0, 143.5, 128.0, and 22.8 ppm. IR (KBr): 3235 3180 2999 2771 1683 1590 1543 1498 1424 1363 1346 1257 1243 1111 1041 1001 899 747 714 652 590 cm^{-1}. Elemental analysis calcd for $C_{12}H_{12}N_9O_9$ (384.26): C 37.51, H 3.15, N 21.87 %; found C 37.36, H 3.24, N 21.71 %.

1,3,5-Trinitro-2,4,6-trinitroaminobenzene (TNTNB)

As-prepared **1** (0.40 g, 1.04 mmol) was dispersed into trifluoroacetic acid (3 ml) at −10°C, and fuming nitric acid (1 ml) was slowly added into the mixture, which was then stirred at −10° to 0°C. The precipitate generated about 1.5 to 2.0 hours, filtered out, and washed carefully with trifluoroacetic acid (1 ml) and dichloromethane (2 ml) to get TNTNB (0.23 g, 56.3% yield). ^{1}H NMR (CD_3CN-d_3, 500 MHz): δ 10.48 (s) ppm. ^{13}C NMR (CD_3CN-d_3, 125 MHz): δ 147.3 and 126.2 ppm. ^{15}N NMR (MeOD-d_4, 500 MHz): δ 357.00, 348.34, and 180.74 ppm. IR (KBr): 3283 1597 1547 1440 1384 1344 1308 1122 1109 992 927 912 815 754 741 717 562 cm^{-1}. Elemental analysis calcd for $C_6H_3N_9O_{12}$ (393.14): C 18.33, H 0.77, N 32.07 %; found C 18.16, H 0.82, N 32.20 %.

Triammonium 1,3,5-trinitro-2,4,6-trinitroamidebenzene (3-[TNTNB^{3-}][3NH4^{+}])

A total of 28% aqueous ammonia solution (0.19 g, 1.6 mmol) was added into the solution of TNTNB (0.20 g, 0.5 mmol) in acetonitrile. After being stirred for another 30 min, the precipitate was filtered to get **3** (0.21 g, 94.5% yield). ^{1}H NMR (DMSO-d_6, 500 MHz): δ 7.14 (s) ppm. ^{13}C NMR (DMSO-d_6, 125 MHz): δ 136.7 and 134.4 ppm. ^{15}N NMR (DMSO-d_6, 500 MHz): δ 368.21, 364.11, 239.39, and 22.16 ppm. IR (KBr): 3584 3202 3026 1575 1522 1404 1366 1331 1306 1283 1247 1138 1023 977 928 811 768 702 677 617 cm^{-1}. Elemental analysis calcd for $C_6H_{12}N_{12}O_{12}$ (444.23): C 16.22, H 2.72, N 37.84 %; found C 16.11, H 2.89, N 37.72 %.

Trihydrazinium 1,3,5-trinitro-2,4,6-trinitroamidebenzene (4-[TNTNB^{3-}][3N2H5^{+}])

A total of 80% aqueous hydrazine solution (0.10 g, 1.6 mmol) was added into the solution of TNTNB (0.20 g, 0.5 mmol) in acetonitrile. After being stirred for another 30 min, the precipitate was filtered to get **4** (0.22 g, 89.9% yield). ^{1}H NMR (DMSO-d_6, 500 MHz): δ 5.80 (s) ppm. ^{13}C NMR (DMSO-d_6, 125 MHz): δ 136.8 and 134.5 ppm. ^{15}N NMR (DMSO-d_6, 500 MHz): δ 369.24, 364.61, 240.25, and 49.24 ppm. IR (KBr): 3597 3493 3343 3140 3054 2949 2687 1569 1517 1417 1349 1310 1256 1085 1026 984 939 850 775 744 714 607 585 cm^{-1}. Elemental analysis calcd for $C_6H_{15}N_{15}O_{12}$ (489.28): C 14.73, H 3.09, N 42.94 %; found C 14.88, H 3.17, N 42.79 %.

X-ray crystallography

A yellow plate crystal (TNTNB) of dimensions 0.20 × 0.15 × 0.02 mm^3, a yellow block crystal (TNTNB·5H_2O·EtOH) of dimensions 0.13 × 0.12 × 0.10 mm^3, a yellow plate crystal (TNTNB·2H_2O) of dimensions 0.20 × 0.18 × 0.01 mm^3, a colorless block crystal (**1**) of dimensions 0.20 × 0.20 × 0.10 mm^3, a yellow block crystal (**3**·3H_2O) of dimensions 0.13 × 0.12 × 0.10 mm^3, and a yellow block crystal (**4**·H_2O) of dimensions 0.10 × 0.10 × 0.10 mm^3 were mounted on an Enraf-Nonius CAD4 four-circle diffractometer using graphite-monochromated Mo Ka radiation (λ = 0.71073 Å) at 153 to 296 K. Corrections for Lorentz and polarization effects and for absorption (ψ scan) were applied.

SUPPLEMENTARY MATERIALS

Supplementary material for this article is available at https://science.org/doi/10.1126/sciadv.abn3176

REFERENCES AND NOTES

1. H. E. Armstrong, The faraday benzene Centenary1. *Nature* **115**, 1010–1013 (1925).
2. J. A. Smith, K. B. Wilson, R. E. Sonstrom, P. J. Kelleher, K. D. Welch, E. K. Pert, K. S. Westendorff, D. A. Dickie, X. Wang, B. H. Pate, W. D. Harman, Preparation of cyclohexene isotopologues and stereoisotopomers from benzene. *Nature* **581**, 288–293 (2020).
3. Y. Segawa, M. Kuwayama, Y. Hijikata, M. Fushimi, T. Nishihara, J. Pirillo, J. Shirasaki, N. Kubota, K. Itami, Topological molecular nanocarbons: All-benzene catenane and trefoil knot. *Science* **365**, 272–276 (2019).
4. S. Suzuki, Y. Segawa, K. Itami, J. Yamaguchi, Synthesis and characterization of hexaarylbenzenes with five or six different substituents enabled by programmed synthesis. *Nat. Chem.* **7**, 227–233 (2015).
5. P. Wang, P. Verma, G. Xia, J. Shi, J. X. Qiao, S. Tao, P. T. W. Cheng, M. A. Poss, M. E. Farmer, K. Yeung, J. Yu, Ligand-accelerated non-directed C–H functionalization of arenes. *Nature* **551**, 489–493 (2017).
6. G. Zhang, B. Hua, A. Dey, M. Ghosh, B. A. Moosa, N. M. Khashab, Intrinsically porous molecular materials (ipms) for natural gas and benzene derivatives separations. *Acc. Chem. Res.* **54**, 155–168 (2021).
7. S. Lee, I. Chataigner, S. R. Piettre, Facile dearomatization of nitrobenzene derivatives and other nitroarenes with n-benzyl azomethine ylide. *Angew. Chem. Int. Ed.* **50**, 472–476 (2011).
8. D. Formenti, F. Ferretti, F. K. Scharnagl, M. Beller, Reduction of nitro compounds using 3d-non-noble metal catalysts. *Chem. Rev.* **119**, 2611–2680 (2019).
9. M. Reichel, D. Dosch, T. M. Klapötke, K. Karaghiosoff, Correlation between structure and energetic properties of three nitroaromatic compounds: Bis(2,4-dinitrophenyl) ether, bis(2,4,6-trinitrophenyl) ether, and bis(2,4,6-trinitrophenyl) thioether. *J. Am. Chem. Soc.* **141**, 19911–19916 (2019).
10. J. C. Bennion, A. J. Matzger, Development and evolution of energetic cocrystals. *Acc. Chem. Res.* **54**, 1699–1710 (2021).
11. Y. Wang, Y. Liu, S. Song, Z. Yang, X. Qi, K. Wang, Y. Liu, Q. Zhang, Y. Tian, Accelerating the discovery of insensitive high-energy-density materials by a materials genome approach. *Nat. Commun.* **9**, 2444 (2018).
12. M. L. Hause, N. H. Herath, R. Zhu, M. C. Lin, A. G. Suits, Roaming-mediated isomerization in the photodissociation of nitrobenzene. *Nat. Chem.* **3**, 932–937 (2011).
13. O. T. O'Sullivan, M. J. Zdilla, Properties and promise of catenated nitrogen systems as high-energy-density materials. *Chem. Rev.* **120**, 5682–5744 (2020).
14. T. M. Klapötke, Chemistry of high-energy materials, III edition; De Gruyter: Boston, (2015).
15. J. R. Deschamps, D. A. Parrish, Stabilization of nitro-aromatics. *Propellants Explos. Pyrotech.* **40**, 506–513 (2015).
16. J. Wilbrand, Trinitrotoluene. *Ann. Chem.* **12**, 178–179 (1863).
17. Z. A. Akopyan, Y. T. Struchkov, V. G. Dashevskii, Crystal and molecular structure of hexanitrobenzene. *Zhurnal Strukturnoi Khimii.* **7**, 385–392 (1966).
18. H. Zong, C. Yao, C. Sun, J. Zhang, L. Zhang, Structure and stability of aromatic nitrogen heterocycles used in the field of energetic materials. *Molecules* **25**, 3232 (2020).
19. M. H. Keshavarz, Simple correlation for predicting detonation velocity of ideal and non-ideal explosives. *J. Hazard. Mater.* **166**, 762–769 (2009).
20. C. Zhang, F. Jiao, H. Li, Crystal engineering for creating low sensitivity and highly energetic materials. *Cryst. Growth Des.* **18**, 5713–5726 (2018).
21. A. T. Nielsen, R. L. Atkins, W. P. Norris, C. L. Coon, M. E. Sitzmann, Synthesis of polynitro compounds. Peroxydisulfuric acid oxidation of polynitroarylamines to polynitro aromatics. *J. Org. Chem.* **45**, 2341–2347 (1980).
22. R. L. Atkins, A. T. Nielsen, C. Bergens, W. S. Wilson, Synthesis of polynitrobenzenes. oxidation of polynitroanilines and their N-hydroxy, N-methoxy, and N-acetyl derivatives. *J. Org. Chem.* **49**, 503–507 (1984).
23. R. L. Atkins, R. A. Hollins, W. S. Wilson, Synthesis of polynitro compounds-hexasubstituted benzenes. *J. Org. Chem.* **51**, 3261–3266 (1986).
24. A. T. Nielsen, R. L. Atkins, Norries, Oxidation of poly(nitro)anilines to poly(nitro)-benzenes. Synthesis of hexanitrobenzene and pentanitrobenzene. *J. Org. Chem.* **44**, 1181–1182 (1979).
25. A. T. Nielsen, A. P. Chafin, S. L. Christian, Nitrocarbons: 4. Reaction of polynitrobenzenes with hydrogen halides-formation of polynitrohalobenzenes. *J. Org. Chem.* **49**, 4575–4580 (1984).
26. Z. Xu, G. Cheng, H. Yang, X. Ju, P. Yin, J. Zhang, J. M. Shreeve, A facile and versatile synthesis of energetic furazan-functionalized 5-nitroimino-1,2,4-triazoles. *Angew. Chem. Int. Ed.* **56**, 5877–5881 (2017).
27. T. M. Klapötke, C. Petermayer, D. G. Piercey, T. M. Stierstorfer, 1,3-Bis(nitroimido)-1,2,3-triazolate anion, the n-nitroimide moiety, and the strategy of alternating positive and negative charges in the design of energetic materials. *J. Am. Chem. Soc.* **134**, 20827–20836 (2012).
28. W. Zhang, J. Zhang, M. Deng, X. Qi, F. Nie, Q. Zhang, A promising high-energy-density material. *Nat. Commun.* **8**, 181 (2017).
29. P. Yin, J. M. Shreeve, From N-nitro to N-nitroamino: Preparation of high-performance energetic materials by introducing nitrogen-containing ions. *Angew. Chem. Int. Ed.* **54**, 14513–14517 (2015).
30. G. Bélanger-Chabot, M. Rahm, R. Haiges, K. O. Christe, Ammonia-(Dinitramido)boranes: High-energy-density materials. *Angew. Chem. Int. Ed.* **54**, 11730–11734 (2015).
31. R. Bu, Y. Xiong, X. Wei, H. Li, C. Zhang, Hydrogen bonding in CHON-containing energetic crystals: A review. *Cryst. Growth Des.* **19**, 5981–5997 (2019).
32. H. Huang, J. Zhong, X. Tan, X. Guo, B. Yuan, Y. Lin, J. S. Francisco, X. Zeng, New insights into the stability of anhydrous 2H-imidazolium fluoride and its high dissolution capability toward a strongly hydrogen-bonded compound. *J. Am. Chem. Soc.* **142**, 10314–10318 (2020).
33. C. L. Jackson, J. F. Wing, On tribromtrinitrobenzol. *Am. Chem. J.* **10**, 283–294 (1888).
34. The crystal data of HNB was cited from the Cambridge Crystallographic Data Centre with CCDC number of 1177301.
35. L. F. Cheung, G. S. Kocheril, J. Czekner, L. Wang, Observation of möbius aromatic planar metallaborocycles. *J. Am. Chem. Soc.* **142**, 3356–3360 (2020).
36. Y. Wang, S. Li, Y. Li, R. Zhang, D. Wang, S. Pang, A comparative study of the structure, energetic performance and stability of Nitro-NNO-azoxy substituted explosives. *J. Mater. Chem. A* **2**, 20806–20813 (2014).
37. H. L. Schmider, A. D. Becke, Chemical content of the kinetic energy density. *J. Mol. Struct.* **527**, 51–61 (2000).
38. The program was downloaded via the following website: https://community.chocolatey.org/packages/crystalexplorer.
39. M. J. Kamlet, S. Jacobs, Chemistry of detonations. I. A simple method for calculating detonation properties of C-H-N-O explosives. *J. Chem. Phys.* **48**, 23–35 (1968).
40. L. N. McHugh, M. J. McPherson, L. J. McCormick, S. A. Morris, P. S. Wheatley, S. J. Teat, D. McKay, D. M. Dawson, C. E. F. Sansome, S. E. Ashbrook, C. A. Stone, M. W. Smith, R. E. Morris, Hydrolytic stability in hemilabile metal-organic frameworks. *Nat. Chem.* **10**, 1096–1102 (2018).
41. K. Cui, S. Bhattacharyya, S. Nair, J. R. Schmidt, Origins of acid-gas stability behavior in zeolitic imidazolate frameworks: The unique high stability of ZIF-71. *J. Am. Chem. Soc.* **143**, 18061–18072 (2021).
42. L. Hu, P. Yin, G. Zhao, C. He, G. H. Imler, D. A. Parrish, H. Gao, J. M. Shreeve, Conjugated energetic salts based on fused rings: Insensitive and highly dense materials. *J. Am. Chem. Soc.* **140**, 15001–15007 (2018).
43. J. Zhang, Y. Feng, Y. Bo, R. J. Staples, J. Zhang, J. M. Shreeve, One step closer to an ideal insensitive energetic molecule: 3,5-diamino-6-hydroxy-2-oxide-4-nitropyrimidone and its derivatives. *J. Am. Chem. Soc.* **143**, 12665–12674 (2021).
44. The crystal data of TATB was cited from the Cambridge Crystallographic Data Centre with CCDC number of 1266837.
45. M. J. Frisch, G. W. Trucks, H. B. Schlegel, G. E. Scuseria, M. A. Robb, J. R. Cheeseman, G. Scalmani, V. Barone, G. A. Petersson, H. Nakatsuji, X. Li, M. Caricato, A. Marenich, J. Bloino, B. G. Janesko, R. Gomperts, B. Mennucci, H. P. Hratchian, J. V. Ortiz, A. F. Izmaylov, J. L. Sonnenberg, D. Williams-Young, F. Ding, F. Lipparini, F. Egidi, J. Goings, B. Peng, A. Petrone, T. Henderson, D. Ranasinghe, V. G. Zakrzewski, J. Gao, N. Rega, G. Zheng, W. Liang, M. Hada, M. Ehara, K. Toyota, R. Fukuda, J. Hasegawa, M. Ishida, T. Nakajima, Y. Honda, O. Kitao, H. Nakai, T. Vreven, K. Throssell, J. A. Montgomery, Jr., J. E. Peralta, F. Ogliaro, M. Bearpark, J. J. Heyd, E. Brothers, K. N. Kudin, V. N. Staroverov, T. Keith, R. Kobayashi, J. Normand, K. Raghavachari, A. Rendell, J. C. Burant, S. S. Iyengar, J. Tomasi, M. Cossi, J. M. Millam, M. Klene, C. Adamo, R. Cammi, J. W. Ochterski, R. L. Martin, K. Morokuma, O. Farkas, J. B. Foresman, D. J. Fox, Gaussian 09, Revision a.02; Gaussian, Inc. Wallingford, CT (2009).
46. T. Lu, F. Chen, Multiwfn: A multifunctional wavefunction analyzer. *J. Comput. Chem.* **33**, 580–592 (2012).
47. The heats of detonation of TNT, PA, RDX, and HMX were cited from (*14*), and the heats of detonation of salt 3, salt 4, CL-20, HNB, and TNTNB were obtained at the same level (see Supporting Information).
48. N. Fischer, D. Fischer, T. M. Klapötke, D. G. Piercey, T. M. Stierstorfer, Pushing the limits of energetic materials – The synthesis and characterization of dihydroxylammonium 5,5′-bistetrazole-1,1′-diolate. *J. Mater. Chem.* **22**, 20418–20422 (2012).
49. M. Deng, Y. Feng, W. Zhang, X. Qi, Q. Zhang, A green metal-free fused-ring initiating substance. *Nat. Commun.* **10**, 1339 (2019).
50. L. M. Kostkova, E. A. Miroshnichemko, Y. N. Matyushin, Inter Ann Conf. of ICT, 31st. p. 50/1–50/11, Karlsruhe, Germany (2000).
51. P. J. Linstrom, W. G. Mallard, W. G. NIST Chemistry WebBook, NIST Standard Reference Database Number 69, website: http://webbook.nist.gov (2021).

Acknowledgments
Funding: This work was financially supported by the National Natural Science Foundation of China (nos. 21875021 and 22075024) and China Postdoctoral Science Foundation (no. 2020 M680391). **Author contributions:** Q.S., S.L., and S.P. designed the study. Q.S., N.D., C.Z., and Q.Z. performed the experiments and characterizations. Q.S., N.D., and S.Z. conducted the calculations and mechanism investigation. Q.S. and S.L. prepared the original draft of the manuscript, which was then reviewed and edited by S.P. All the authors discussed the results of the paper. **Competing interests:** The authors declare that they have no competing interests. **Data and materials availability:** All data needed to evaluate the conclusions in the paper are present in the paper and/or the Supplementary Materials.

Submitted 18 November 2021
Accepted 3 February 2022
Published 23 March 2022
10.1126/sciadv.abn3176

ScienceAdvances

Full-nitro-nitroamino cooperative action: Climbing the energy peak of benzenes with enhanced chemical stability

Qi SunNing DingChaofeng ZhaoQi ZhangShaowen ZhangShenghua LiSiping Pang

Sci. Adv., 8 (12), eabn3176. • DOI: 10.1126/sciadv.abn3176

Science Advances (ISSN) is published by the American Association for the Advancement of Science. 1200 New York Avenue NW, Washington, DC 20005. The title *Science Advances* is a registered trademark of AAAS.